Scaling of ion spectral peaks in a hybrid RPA-TNSA regime

K. F. Kakolee

Institute of Basic Science (IBS), Centre for Relativistic Laser Science (CoReLs), 123 Cheomdan gwagiro, Buk gu, Gwangju 500-712, Korea.

M. Borghesi, M. Zepf, S. Kar, D Doria, B. Ramakrishna, K. Quinn, G. Sarri,

School of Mathematics and Physics, Queen's University of Belfast, Belfast, BT7 1NN, U. K.

J. Osterholz, M. Cerchez, O. Willi

Institut f¨ur Laser-und Plasmaphysik, Heinrich-Heine-Universit¨at, D¨usseldorf, GermanyHeinrich Heine-Universitat Dusseldorf, Germany.

X. Yuan, P. McKenna

Department of Physics, SUPA, University of Strathclyde, Glasgow G4 0NG, UK.

The role of the radiation pressure of an intense laser beam in the formation of proton and carbon spectra from thin foils has been discussed. The data presented suggests that the onset of the Light Sail regime of Radiation Pressure Acceleration can be obtained, for suitably thin targets, at currently available laser intensities, in competition with the Target Normal Sheath Acceleration mechanism. The spectral features and their scaling with the laser and target parameters, are consistent with the scenario of LS acceleration.

PACS number: 52.38.Kd, 41.75.Jv

Keywords: Hybrid RPA-TNSA, Scaling of ion.

Email: kakolee_kaniz@yahoo.com

Fax: +82-62-715-4705

1. INTRODUCTION

Laser-driven ion acceleration has been a rapidly progressing field of great interest since the first observations [1] of energetic ion beams from laser irradiated foil targets. High quality ion beams have many prospective applications in scientific, technological and medical areas such as medical isotope production, tumour therapy, ultrafast radiography and laser-driven fusion [2]. For the interaction of a laser with solid-density targets, several ion acceleration mechanisms have been identified and investigated. Among them the two most discussed are Target Normal Sheath Acceleration (TNSA) and Radiation Pressure Acceleration (RPA).

Ion beams with energies of several tens of MeV have been obtained in experiments via the TNSA mechanism [1, 3, 4], where the ions are driven by the sheath fields established at the target rear surface, due to the relativistic electrons produced at the target front surface during the intense laser interaction. However, low particle density, large divergence, and almost 100% energy spread of the proton beam poses significant limitations for many of the envisioned applications, for instance hadron therapy of deep-seated cancers. By contrast, ion beam production by the radiation pressure of intense lasers has been predicted to be a promising route for accelerating large numbers of ions quasi-monoenergetically to "relativistic" energies (GeV/nucleon range), in a significantly more efficient manner compared to TNSA [5-7].

There are two regimes of RPA, viz. hole-boring (HB) and Light sail (LS), which have been identified by simulations and recent experimental results [8]. In the RPA mechanism, ions are accelerated by directional momentum transfer from laser to target via the laser's ponderomotive force, which acts as a snow-plow on the target front surface and launches a dense ion bunch into the target. The radiation pressure instantly pushes the electrons in the skin depth which sets a strong accelerating field for ions to follow promptly the electrons. Consequently, the laser pulse bores through the target (Hole-boring (HB) regime) where the ion front velocity (*hole boring velocity*) depends on the laser intensity (I) and target mass density (ρ). If the target thickness is less than the product of the laser pulse duration and hole boring velocity, the ions will pile up at the target rear surface before the end of the laser pulse. As the thickness of the compressed layer becomes comparable or less than the evanescence length of the ponderomotive force, the whole layer is cyclically accelerated with high efficiency for the rest of the duration of the intense laser pulse. The latter scenario of whole foil acceleration is called *light-sail* regime.

In the experiment mentioned here, both the Hole boring (HB) and Light sail (LS) regimes of RPA have been extensively explored employing the Vulcan Petawatt laser. For thick targets, where the product of the HB velocity and the laser pulse duration is less than the target thickness, collimated ion jets were observed, emerging from the rear surface of the targets over a hydrodynamic time scale [9]. On the other hand, for sufficiently thin targets, the LS mechanism resulted in narrow band heavy ion spectra with energy up to 20 MeV/nucleon, which is discussed in this report. The scaling for ion energy is obtained by varying the laser and target parameters over several shots.

II. EXPERIMENT

The experiment was carried out using the VULCAN Nd:glass laser, operating in chirped pulse amplification (CPA) mode. The laser wavelength and full width at half maximum (FWHM) pulse duration are 1.053 μm and 750 fs respectively. The laser was focused down on the target at near normal incidence by using an *f*/3 off-axis parabola. In order to reduce the pre-pulses and to suppress the intensity of amplified spontaneous emission, a plasma mirror was employed before the target. A schematic of the experimental setup is shown in the Fig. 1. A zero order quarter wave plate was used in the focusing beam, before the plasma mirror, in order to change the polarisation of the laser on the target. The intensity on the target was varied from 5×10^{19} W/cm^2 to 3×10^{20} W/cm^2 by increasing the laser spot size on the target, by translating the parabola along the focussing axis. Targets of various materials (Cu, Al, Au and CH) and thickness (10 μm down to 100 nm thickness) were used.

Thomson Parabola Spectrometers (TP –Spec) were employed as the main diagnostic for measuring spectra of multi-MeV ions produced by the interaction. Two high resolutions TP Spec were fielded, one along the laser axis (TP1) and the other looking at 13 ± 2 degree off axis (TP2). Image plates (IP) were used as detectors to record the spectra. IP were cross calibrated with solid state nuclear track detector (CR39) for absolute particle number determination.

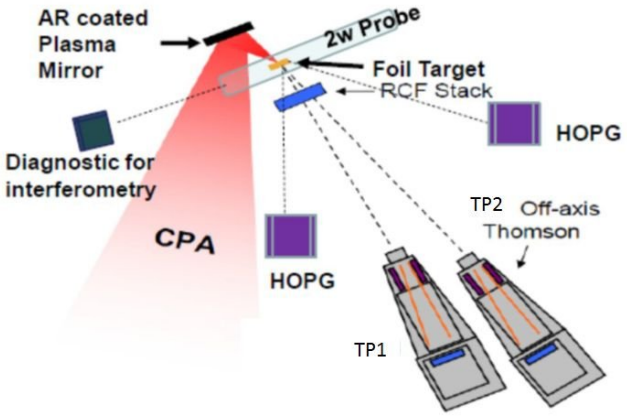

Figure 1. Schematic of the experimental set up.

The energy resolved spatial flux profile of protons was diagnosed by using stacks of radiochromic films (RCF) placed in the bottom half of the beam.

III. RESULT AND DISCUSSIONS

Spectra of accelerated ions of different species resulting from the interaction were diagnosed for different laser and target parameters over many shots. We detected not only ions of the main target components, but also, as usual in these experiments, several other ion species such as C, O, H present in surface contaminant layers. Instead of the quasi maxwellian energy spectra typically observed in case of TNSA, the spectra from thin targets contains a peaked feature towards the higher energy side.

Since for the thin targets, the HB accelerated ions from the target front surface are expected to reach the target rear surface in less than the laser pulse duration (0.1 ps for the case shown in the fig. 2(a)), the remaining duration of the CPA pulse is spent in accelerating the ions in the LS regime. We believe that this is the cause of the peaked spectral feature observed in the spectra. On the other hand, for thicker targets we obtained exponential ion spectra (fig. 2 (b))

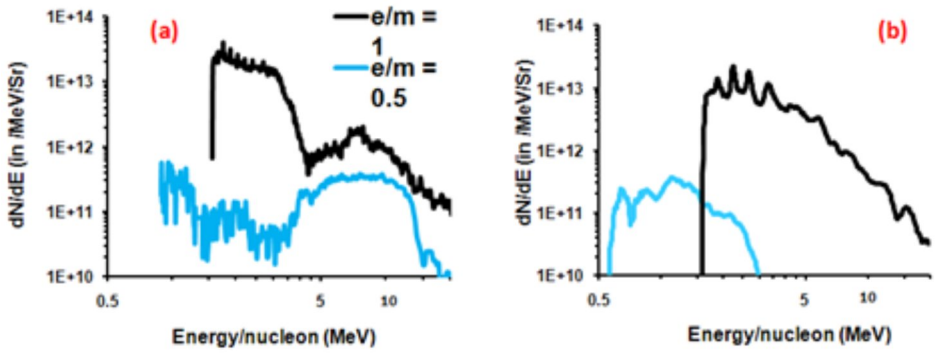

Fig 2. Experimental obtained spectra of two ion species for (a) thin (100 nm) and (b) thick (10 um) Cu targets irradiated at similar laser intensity of $3 \times 10^{20} W/cm^2$. Thses spectra are from TP1.

typical to TNSA mechanism. It is most likely that the proton spectral profile in fig. 2(a) results from the overlap of a narrow band proton spectrum originated by the LS mechanism, with an exponential spectrum by TNSA mechanism taking place over an extended area (of several 100s of micron) on the target rear surface, due to recirculation of hot electrons [10]. However, such an exponential feature is not prominent in the spectra for the species with e/m=0.5 (which could correspond to fully ionized Carbon), as protons get preferentially accelerated by the TNSA mechanism. The dominance of proton acceleration in a "pure" TNSA scenario can in fact be seen in the fig. 2(b).

In order to assess the possible influence of Radiation Pressure effects on the spectral profiles observed here, a simple analytical model was developed taking into account the HB and LS phases of RPA mechanism. Because of the extreme radiation pressure (of the order of 100s of GBar) exerted on the irradiated target surface, ions are swept forward by directional momentum transfer. The ion equation of motion, in the scenario of whole foil acceleration (LS regime) can be expressed by equation [7, 11, 12],

$$\gamma^3 \frac{d\beta_{LS}}{d\tau} = \frac{2m_e a_o (\tau - \dot{x})^2}{m_p \chi} \left(\frac{1-\beta_{LS}}{1+\beta_{LS}}\right) R(\beta_{LS}) \qquad (1)$$

where

$$\beta_{LS} = \frac{(1+\psi)^2 - 1}{(1+\psi)^2 + 1}, \text{ where } \psi = 2\pi \frac{Z}{A} \frac{m_e}{m_p} \frac{a_o^2}{\zeta} \tau_{ls}$$

Here, $a_o(\tau) = 0.85\sqrt{I_o(\tau - x`)\lambda^2/10^{18} W cm^{-2}}$ is the dimensionless laser amplitude; $\rho` = \frac{\rho}{m_p n_c}$. $I_o(\tau - x`)$ is the laser intensity on axis as a function of retarding time, $\tau - x`$ where $\tau = \frac{ct}{\lambda}$ and $\gamma = (1 - \beta_{LS}{}^2)^{\frac{-1}{2}}$, $\chi = \frac{\rho` l}{\lambda}$ for a target thickness l, under the approximation that the areal density of the compressed layer is same as that of the target before the interaction. The term $R(\beta_{LS})$ is the non-linear intensity reflection coefficient given by Eq.[19] in the ref. [12 (b)]. Using the laser and target parameters relevant to the case shown in the Fig. 2(a) in a simple numerical model based on the equation (1), we found that an ion energy of 8 MeV/nucleon is expected by the LS mechanism, which agrees well with the experimental data (see the data point "A" in the Fig. 3).

The scaling of the spectral peak has been obtained by a methodical scan over a range of target thickness, density, laser intensity and polarization. Fig 3 shows the energy scaling of the ion

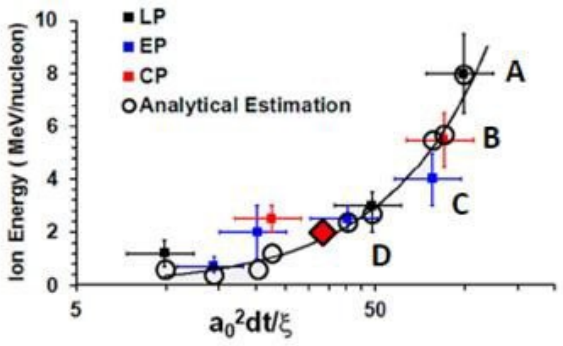

Fig 3(a). Graph showing the peak energy (/nucleon) of the ion species with e/m=0.5. The red diamond with the black outer line represents the previously reported experimental data by Henig et. al. [8 (a)]. The experimental parameter set (intensity, target material, target thickness) for the data points marked as A, B, C and D are (3×10^{20} W/cm^2, Cu, 0.1μm), (1.25×10^{20} W/cm^2, Cu, 0.05μm), (2.2×10^{20} W/cm^2, Cu, 0.1μm), (6×10^{19} W/cm^2, Al, 0.1μm) respectively. The experimental parameter set [a_0, target material, target thickness(μm)] for the data points after D from right to left are [13.8, Cu, 0.1], [7.5, Al, 0.1], [6.9, Al, 0.1], [13.6, Al, 0.5] and [14.1, Al, 0.8] respectively. The circles represent the results from simple numerical modelling based on the eq. (1) (which comes from the equation of motion in LS regimes from [7, 11-12, 14-15]). Data point "A" corresponds to the case shown in the Fig. 2(a).

peak with the relevant scaling parameter $a_o^2\tau_{LS}/\zeta$. We can also see that, there is a good agreement between experimental data and RPA estimations. The experimental data points show that the ion energy scales with $(a_o^2\tau_{LS}/\zeta)^{1.5}$, which is significantly faster than the TNSA scaling $E \infty a_o$.

Since the narrow-band spectral features were observed along the laser axis and were not observed in TP2 (13±2 deg off axis Thompson), this indicates an emission cone of less than 13±2 deg. This clearly suggests that the underlying mechanism produces a relatively narrow bandwidth spectrum with smaller divergence cone angle than that of a TNSA accelerated beam. This indication is corroborated by the RCF stack data, as shown in the fig. 4 (a), taken simultaneously with the spectral measurement by TPs. Typically in each shot taken in the

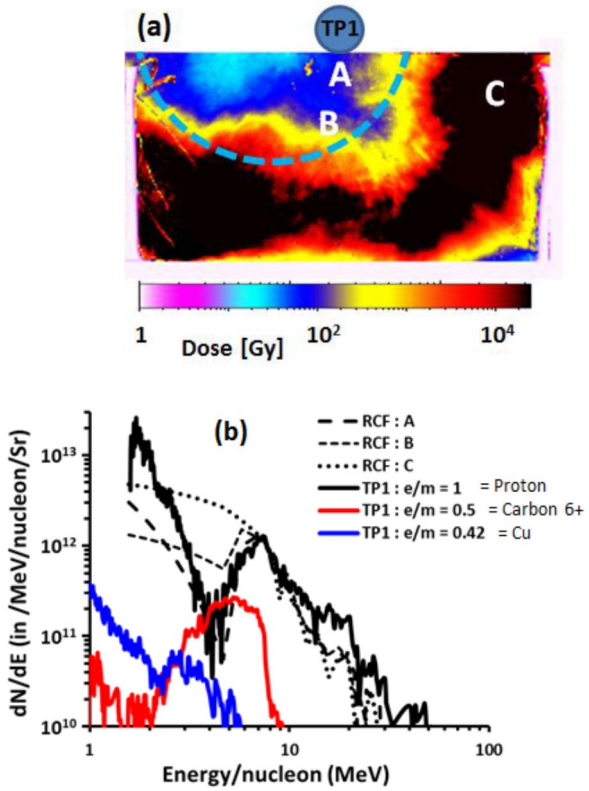

Figure 4 *(a) RCF image showing dose distribution in the lower half of the proton beam, deposited mainly by 5 MeV protons, 50 nm Cu targets irradiated by a CP laser pulse at peak intensity of* $1.25 \times 10^{20}\ W/cm^2$. *(b) For the same shot, the graph shows comparison between the proton spectra obtained from the TP1 and the spectra at different locations in the RCF marked as letters A, B and C.*

experiment, the relatively narrow band spectral feature appears (along the laser axis) simultaneously for proton and carbon species. Therefore, a spatially and spectrally resolved profile of the proton beam was captured in another shot employing a RCF stack as shown in the fig. 4 (a). The spatially resolved proton beam profiles produce information on the divergence in addition to the dose distribution. As the stopping range of carbon is significantly shorter than for protons at the same energy/nucleon (for example, stopping range of 5 MeV/nucleon proton and carbon in mylar are 300 μm and 100 μm respectively), on the basis of the TP spectra observed, the deposited dose in the RCFs in the stack (wrapped with 30 μm Aluminum foil to avoid the laser debris) can be assumed to be primarily due to the protons. The proton spectrum from the RCFs was reproduced by deconvolution method. Fig. 4 (b) shows the comparison between the proton spectra obtained from TP1 and the spectra at different locations in the RCF marked by the letters A, B and C. The position of the Thompson spectrometer is denoted by TP. The narrow band feature in the proton spectrum observed in the TP1 was reproduced (dashed line in fig. 4 (b)) for a defined region in the RCF corresponding to a half cone beam divergence of$\sim 10^0$. If we take this as the divergence of the narrow band component of the carbon ion beam, the conversion efficiency into this component can be estimated as 1%, which is significantly higher than reported in [13] and comparable to ref. [8 (a)].

IV. CONCLUSIONS

From the work presented here it is clear that viable schemes exist to enhance the performance of current and future laser driven ion sources, pushing the state of the art closer to that required for many exciting applications.The spectral features, and their scaling with the laser and target parameters, are consistent with the scenario of LS acceleration. To check the possible influence of Radiation Pressure effects on the spectral profiles observed, an analytical model was developed and we found that the peak observed in the ions energy spectra and their scaling with the target and laser parameters are consistent with the expectations for LS.

ACKNOWLEDGMENTS

This work was funded by EPSRC (Engineering and Physical Sciences Research Council) EP/E035728/1 -LIBRA (Laser Induced Beam Radiation and Application) Consortium, EP/J002550/1, U.K. Authors acknowledge the support and contribution of the target fabrication group, the Engineering workshop at CLF (Central Laser Facility), RAL and STFC (Science and Technology Facility Council) Facility access.

REFERENCES

[1] E. L. Clark *et al.,* Phys. Rev. Lett. 84, 670, (2000);A.Maksimchuk et al., ibid. 84, 4108 (2000).

[2] M. Borghesi *et al,* Fusion Science and Technology, 49,412 (2006) and the references therein.

[3] B. M. Hegelich *et al.,* Nature 439, 441 (2006).

[4] H. Schwoerer *et al.,* Nature 439, 445 (2006).

[5] A. Macchi *et al.,* Phys. Rev. Lett. 94, 165003 (2005).

[6] A. P. L. Robinson *et al.,* New. J. Phys. 10, 013021 (2008).

[7] B. Qiao *et al.,* Phys. Rev. Lett. 102, 145002 (2009).

[8] a) A. Henig *et al,* Phys. Rev. Lett. 103, 245003 (2009); b) C. Palmer et al, Phys. Rev. Lett, 106, 014801 (2011).

[9] S. Kar, K.F. Kakolee *et al.,* Plasma Phys. Control. Fusion 55 ,124030, (2013), K. F. Kakolee *et al., CLF-RAL Annual Report (2010).*

[10] F. N¨urnberg *et al.,* Rev. Sci. Instr., **80**, 033301 (2009).

[11] A. Robinson *et al.,* New. J. Phys. 10, 013021 (2008).

[12] (a) A. Macchi *et al.,* Phys. Rev. Lett. 94, 165003 (2005); (b)A. Macchi et. al., New J Phys., 12, 045013 (2010).

[13] D. Jung *et al.*, Phys. Rev. Letts, **107**, 115002 (2011).

[14] A P L Robinson et al., Plasma Phys. Control. Fusion, 51, 024004 (2009).

15] A. Macchi et al., Phys. Rev. Lett, 103, 085003 (2009)